

A comprehensive analysis of the tubarial glands

Alisha Ebrahim¹  | Caitlan Reich^{1,2} | Kurt Wilde³ | Aly Muhammad Salim¹ | Martin D. Hyrcza^{1,2,4} | Lian Willetts^{1,5}

¹Cumming School of Medicine, University of Calgary, Calgary, Alberta, Canada

²Department of Pathology and Laboratory Medicine, University of Calgary, Calgary, Alberta, Canada

³Faculty of Kinesiology, University of Calgary, Calgary, Alberta, Canada

⁴Arnie Charbonneau Cancer Institute, University of Calgary, Calgary, Alberta, Canada

⁵Department of Cell Biology and Anatomy, University of Calgary, Calgary, Alberta, Canada

Correspondence

Lian Willetts, Cumming School of Medicine, University of Calgary, Calgary, AB, Canada.

Email: lian.willetts@ucalgary.ca

Funding information

University of Calgary Department of Pathology and Laboratory Medicine Trainee-Led Project Support Initiative; Department of Cell Biology & Anatomy, Faculty of Medicine, University of Calgary.

Abstract

The tubarial glands (TGs) are a collection of salivary glands (SGs) located within the nasopharynx, proximal to the eustachian tube. Currently, there is no quantitative characterization of the TGs. We investigated the histological architecture of the TGs and compared it with the major and minor SGs for categorization. Tubarial, parotid, submandibular, sublingual, buccal, labial, and lingual glands were excised from human donors (8 male and 3 female). Hematoxylin and eosin-stained tissue sections were analyzed to measure the area of the largest lobule, number of ducts, number of mucinous acini, and mean mucinous acini area. Based on our observation, the TGs' histology resembles the minor SGs, while having some unique characteristics that distinguish them from both major and minor SGs. The area of the largest lobule in the TGs and minor SGs was smaller than the major SGs. TGs have a lower number of ducts than the major and minor SGs. TGs contain densely packed clusters of predominantly mucinous acini surrounded by loose connective tissue resembling minor SGs. This density may explain their previously observed high prostate-specific membrane antigen uptake. In our cohort of donors, sex-based differences were observed in the mean mucinous acini area between male and female TGs, submandibular and sublingual glands. Taken together, our findings suggest the histological characteristics of all SGs are better organized on a spectrum rather than discrete groups (major vs. minor) and provide information to open new avenues for research into the TGs' role in head and neck pathologies and sexual dimorphism of the SGs.

KEYWORDS

salivary glands, sex and gender, tubarial glands

1 | INTRODUCTION

The salivary gland (SG) system plays important roles in lubrication of the oral cavity and pharynx through salivation, which is important for digestion, speaking,

and maintaining a stable pH in the initial portion of the aerodigestive tract (Basbaum et al., 1990). Currently, the human SG system is categorized into the major and the minor glands. The paired parotid, sublingual, and submandibular glands are the major SGs, which are located

This is an open access article under the terms of the [Creative Commons Attribution-NonCommercial-NoDerivs](https://creativecommons.org/licenses/by-nc-nd/4.0/) License, which permits use and distribution in any medium, provided the original work is properly cited, the use is non-commercial and no modifications or adaptations are made.

© 2024 The Author(s). *The Anatomical Record* published by Wiley Periodicals LLC on behalf of American Association for Anatomy.

both extra- and intra-orally and have ducts that empty into the oral cavity. In addition to the major SGs, there are ~1000 minor SGs spread throughout the upper aerodigestive tract (Figure 1a). Histologically, the SGs are composed of networks of acini connected by ducts (Gilloteaux & Afolayan, 2014; Lee et al., 2012; Tucker, 2007). There are 3 classes of acini found in the human

digestive system: serous, mucinous, and seromucinous. The serous acini (Figure 1bI) produce and secrete a watery fluid containing proteins, enzymes, and antibodies to protect the aerodigestive tract. Histologically, the paired parotid glands contain mainly serous acini. The mucinous acini (Figure 1bII) produce and secrete mucins to thicken saliva and protect the mucosal

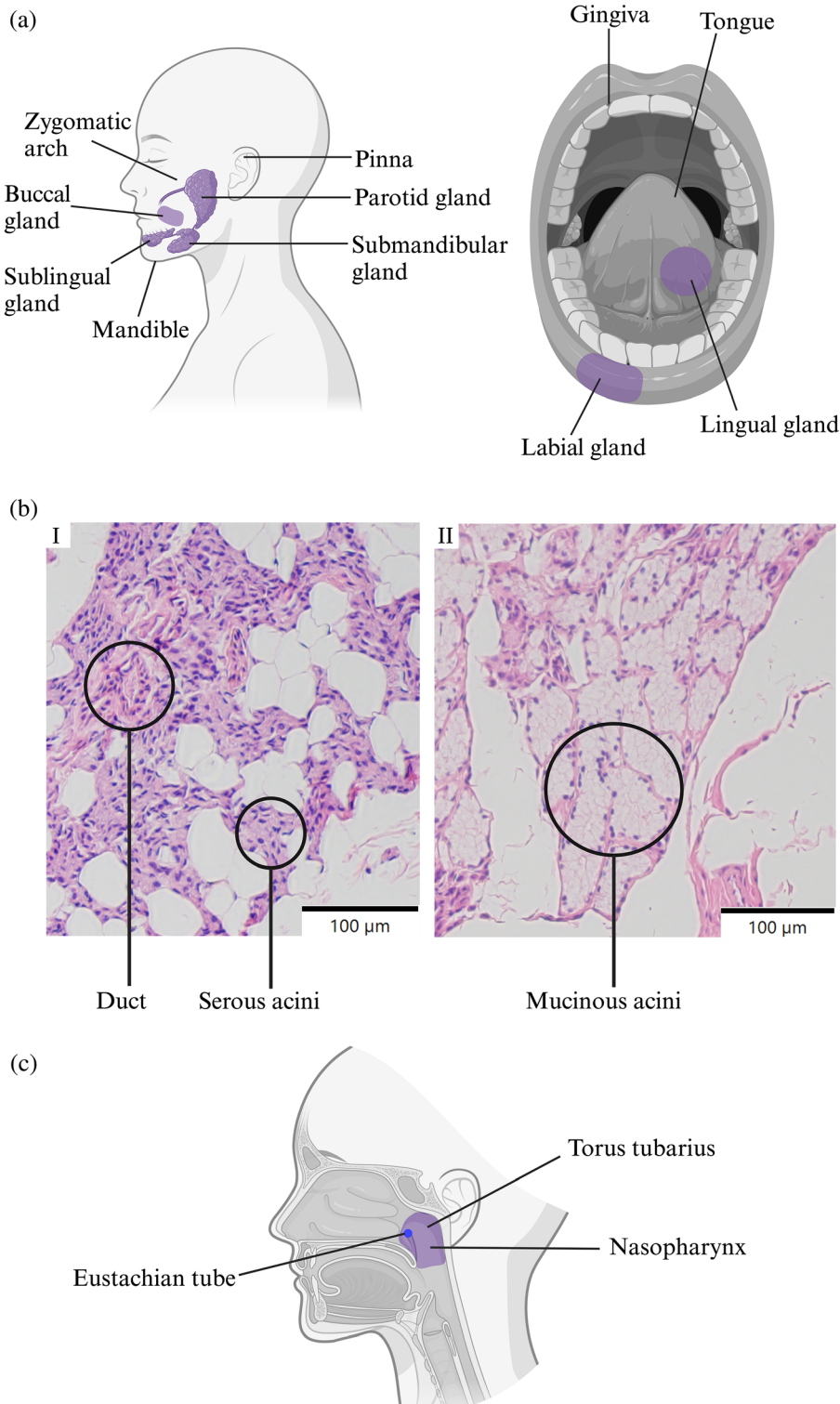


FIGURE 1 Anatomical location and histological structure of the salivary glands (SGs). (a) Anatomical location of the major SGs (parotid, sublingual, and submandibular glands) and the minor SGs that are being studied (buccal, labial, and lingual glands). (bI) Parotid gland with serous acini and a duct surrounded by adipose tissue at 100 \times . (bII) Sublingual gland with mucinous acini adjacent to a duct and connective tissue at 100 \times . Serous acini have a spherical shape and secrete a watery, protein-rich fluid, whereas mucinous acini produce a thick, glycoprotein-rich mucous. Intercalated ducts are made of cuboidal cells and function to transport the fluid produced by acini to the aerodigestive tract. Scale bar is 100 μ m. (c) Anatomical location of the tubarial glands (TGs). The TG is overlaying the torus tubarius region shaded in purple. The TGs are located within the nasopharynx, proximal to the eustachian tube, superior to the soft palate and posterior to the inferior nasal conchae.

surfaces from drying. The sublingual glands contain mainly mucinous acini. The seromucinous acini found in the submandibular glands produce a combination of serous and mucinous fluid (Hsieh et al., 2016). The fluid produced by the acini is drained toward the oral cavity via the excretory ducts (Figure 1b1) (Lee et al., 2012).

The current classification of major and minor SGs is based on a few key characteristics which are neither comprehensive nor quantitative (Kessler & Bhatt, 2018). The major SGs secrete into the oral cavity via an extensively branched system of ducts and have a more highly organized, lobular acini arrangement than minor SGs (Gupta & Ahuja, 2019; Hukkanen et al., 2018). Furthermore, major SGs can be identified on standard radiological images (e.g. magnetic resonance imaging [MRI]). In comparison, minor SGs are comprised of unstructured acini spread throughout the aerodigestive tract and are difficult to visualize on standard radiological images (Gupta & Ahuja, 2019; Kessler & Bhatt, 2018; Tani & Skoog, 2008).

The tubarial glands (TGs) are a set of predominantly mucinous glands located around the torus tubarius within the nasopharynx (Figure 1c) and were previously uncharacterized until recently due to their anatomical location only being clinically accessible through nasal endoscopy. Incidentally, the TGs and all SGs can be visualized using prostate-specific membrane antigen (PSMA) positron emission tomography/computed tomography (PET/CT) scans. Analysis of PSMA PET/CT scans from 100 patients (99 male and 1 female) diagnosed with prostate or paraurethral gland cancer revealed a bilateral area of high PSMA uptake located in the nasopharynx, overlaying the torus tubarius and proximal to the eustachian tube (Valstar et al., 2021). Histological investigation revealed that this area was comprised of SG tissue (Valstar et al., 2021). To date, the anatomical and histological categorizations of the TGs are not comprehensive. Additionally, the functions of the TGs need further investigation, as TG dysfunction could be associated with dry mouth and difficulty swallowing and might also contribute as the source of SG tumors (Turk, 2020; Valstar et al., 2021).

Although the level of PSMA uptake on PET/CT has not been used as a criterion for classification of the SGs, the TGs were proposed to be classified as major SGs based on the similar PSMA PET/CT signal intensity of the TGs and the sublingual glands (Valstar et al., 2021). However, this proposal neglects to consider the histological structure and the gross anatomy of these glands. Furthermore, the incidental visualization of the TGs is biased toward males and does not explore potential sex-based differences. PSMA PET/CT is primarily used for prostate cancer diagnosis and staging, creating a

natural bias against females. No comprehensive analysis of gross quantitative metrics and qualitative descriptions of the TGs in females currently exist. Previous literature has found limited structural and functional differences between male and female SGs; however, no studies have had sex-based histological comparisons (Inoue et al., 2006; Moreira et al., 2006; Rosa et al., 2020). Clinically, understanding the sexual dimorphism of SGs can aid in developing management plans that are closely aligned with the individual's own anatomy, especially if differences in salivation become pronounced as a side effect of radiotherapy (RT) for treating head and neck cancers (Formenti & Demaria, 2009).

In general, there is a paucity of quantitative histological data describing the major and minor SGs, and the TGs. Without a quantitative histological comparison, we are left with only qualitative and gross quantitative comparisons. The limited analysis of the microscopic structure of the SGs hinders our understanding of SGs' function in both the digestive and respiratory systems. This study provides a comprehensive and sex-based histological analysis of the TGs in comparison to the known major and minor SGs to better understand the TGs' tissue structure and function.

2 | METHODS

2.1 | Dissection

Ethical approval for this study was obtained from the Conjoint Health Research Ethics Board of the University of Calgary, Calgary, Alberta, Canada (REB21-0653) on 21 September 2021. Eight male and 3 female human cadavers (Table 1) were lightly embalmed by following a standard protocol in the Advanced Technical Skills Simulation Laboratory (ATSSL) (Anderson, 2006). In brief, the cadavers were

TABLE 1 Donor characteristics.

Donor	Sex	Age	Place of birth	BMI
1	Female	67	Labrador, Canada	22.8
2	Male	86	British Columbia, Canada	21.0
3	Female	96	Georgia, USA	21.0
4	Male	81	Alberta, Canada	20.9
5	Male	89	Alberta, Canada	22.0
6	Male	86	Alberta, Canada	27.0
7	Male	87	Alberta, Canada	17.4
8	Female	88	British Columbia, Canada	26.0

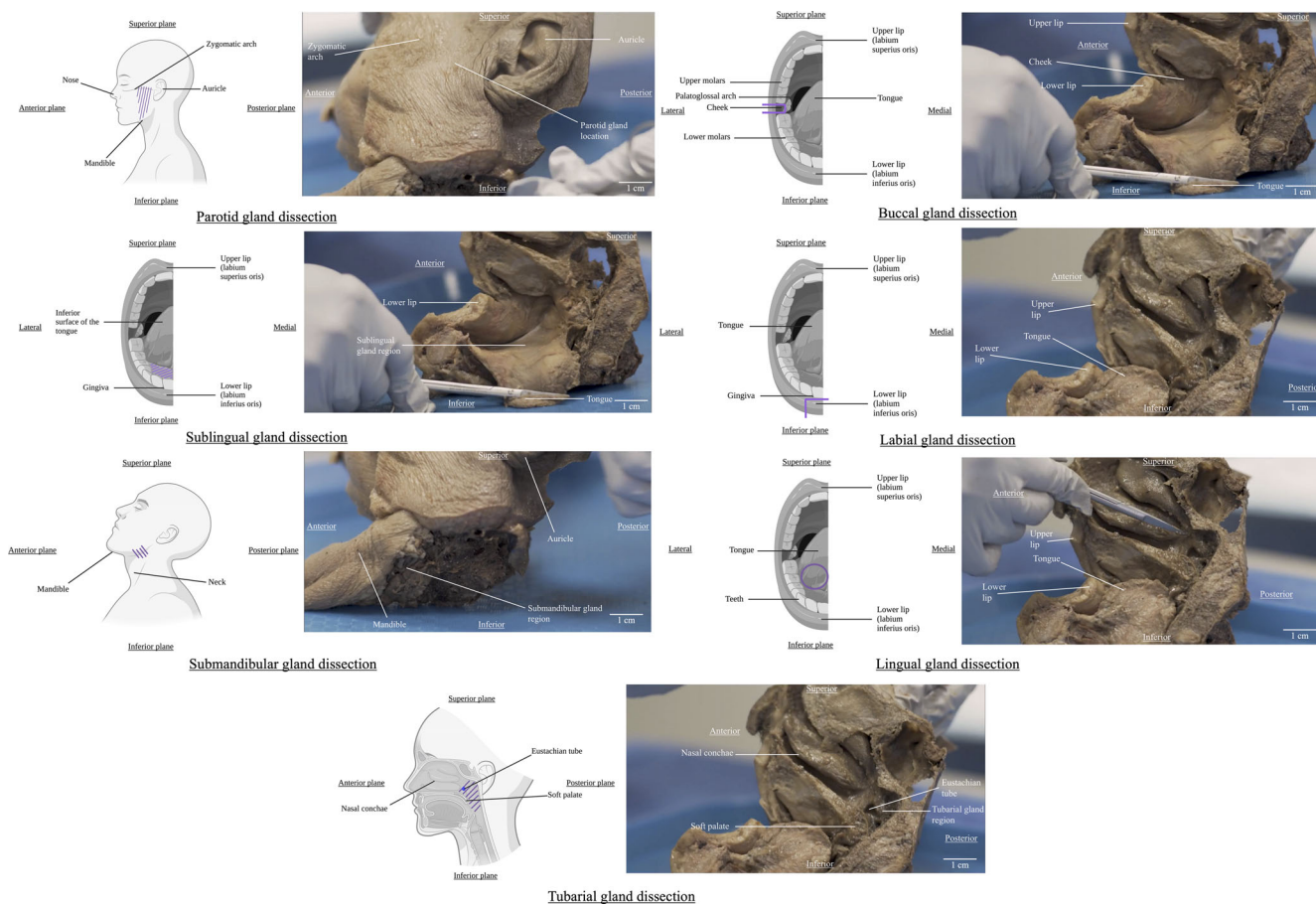


FIGURE 2 Diagrams and images of the gland dissections. The parotid gland was removed by cutting through soft tissue layers proximal to the zygomatic arch and the pinna. The sublingual gland was removed by separating the soft tissue along the gingiva and the inferior surface of the tongue. The submandibular gland was removed by separating the soft tissue inferior to the mandible. Tissue was collected from the cheek intermediate to the lower and upper molars, and lateral to the palatoglossal arch to obtain a sample of the buccal glands; from the lower lip was excised to obtain a sample of the labial glands; and from the ventral tongue was excised to obtain a sample of the lingual glands. The tissue around the eustachian tube, superior to the soft palate and posterior to the nasal conchae was excised to obtain as much tissue from the TG region as possible. Scale bar is 1 cm.

embalmed with formaldehyde-containing soft embalming fluid prior to dissection (Ottone et al., 2016). All dissections were completed bilaterally for maximum specimen availability (Figure 2).

The parotid gland was removed by cutting through muscle and adipose layers proximal to the zygomatic arch and the pinna. The sublingual gland was removed by separating the soft tissue along the gingiva and the inferior surface of the tongue. The submandibular gland was removed by separating the soft tissue inferior to the mandible.

A 3 cm × 3 cm section of tissue was collected from the cheek intermediate to the lower and upper molars, and lateral to the palatoglossal arch to obtain a sample of the buccal glands; from the lower lip was excised to obtain a sample of the labial glands; and from the ventral tongue was excised to obtain a sample of the lingual glands. The tissue around the eustachian tube, superior to the soft palate and posterior to the nasal conchae was

excised to obtain as much tissue from the TG region as possible. The entire TG region was excised as the TGs are not one encapsulated gland that can be excised in toto as with the major SGs. All samples were stored at 8°C in 10 mL vials with 10% formalin for preservation.

All paraffin-embedded glands were serially sectioned with a rotary microtome. Minor SGs were sectioned perpendicularly to the mucosa. Sections were stained with hematoxylin and eosin (H&E) (Washington University School of Medicine Neuromuscular Lab, 1997).

2.2 | Sample analysis

H&E-stained slides were analyzed using a digital light microscope. A representative image showing acini and ducts was taken from each gland at 100× and 400× magnification. Digital images were uploaded to ImageJ software. Comparisons were made between the TGs

and the major and minor SGs, as well as between glandular tissue isolated from male and female donors. For all 11 donors, comparisons were made regarding the mean size of the largest lobule and the number of ducts in 1 high-power field of view (HPF) (100 \times). For 4 (2 male and 2 female) donors, comparisons were made between all glands regarding the number of mucinous acini in 1 HPF, and the mean area of 10 random mucinous acini in 1 HPF. Serous acini were not measured as the borders of each acini were too difficult to discern in the images. Comparisons were also made between male and female glands for those same 4 donors. Lobule size and number of ducts were used as surrogate markers for complexity, providing a bird's eye view of the acinar arrangement and ductal branching of each gland. The number of mucinous acini and area of the mucinous acini provided a close-up description of the structure of each gland. Acini and ducts that were only partially visible due to being cut off at the edge of the field of view were included. Four independent reviewers analyzed all included slides.

Standard descriptive statistics were used to summarize the results. A one-way analysis of variance (ANOVA) and two-tailed unpaired t-tests were used to compare all glands. The significance level is set at $p = 0.05$. Statistical analyses were performed using Stata/IC Version 17.0.

3 | RESULTS

3.1 | Quantitative results

3.1.1 | Sample exclusions

Due to little glandular tissue being found in the tongue dissections of 3 donors, these glands were not included in the quantitative results. The buccal glands from 1 female donor demonstrated higher atrophy than all other samples. The atrophy was evident as the fragile cellular walls of the acini were completely broken down (Data S1). Therefore, this sample was only included in descriptions and calculations regarding the ducts.

TABLE 2 Largest lobule area.

Glands	Mean largest lobule area (standard deviation) (μm^2)
Tubarial glands	5.7×10^5 (3.4×10^5)
Major salivary glands	10.5×10^5 (3.5×10^5)
Minor salivary glands	6.0×10^5 (3.7×10^5)

Note: Data are reported as means and standard deviations. $n = 8$ male donors and 3 female donors.

3.1.2 | Area of the largest lobule

The area of the largest lobule in the major SGs is greater than the TGs ($p < 0.0001$) and minor SGs ($p < 0.0001$). The TGs and minor SGs have similar areas of the largest

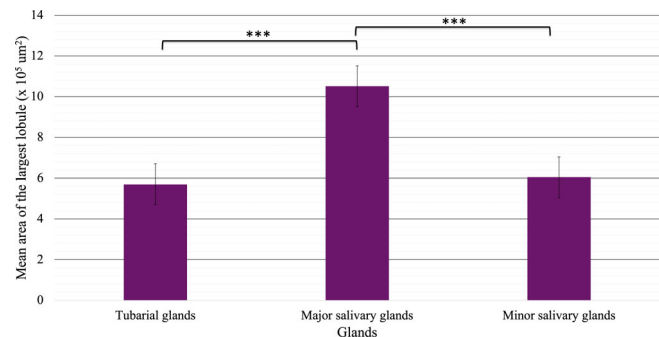


FIGURE 3 Mean area of the largest lobule in one high-power field of view. Major salivary glands have the largest lobules. Data are reported as means and error bars represent standard deviation. $n = 8$ male donors and 3 female donors. A one-way ANOVA was used to compare combined male and female values between all the glands. *** $p < 0.0001$.

TABLE 3 Mean number of ducts.

Glands	Mean number of ducts (standard deviation)
Tubarial glands	3.9 (3.0)
Major salivary glands	21.8 (10.5)
Minor salivary glands	16.2 (11.0)

Note: Data are reported as means and standard deviations. $n = 8$ male donors and 3 female donors.

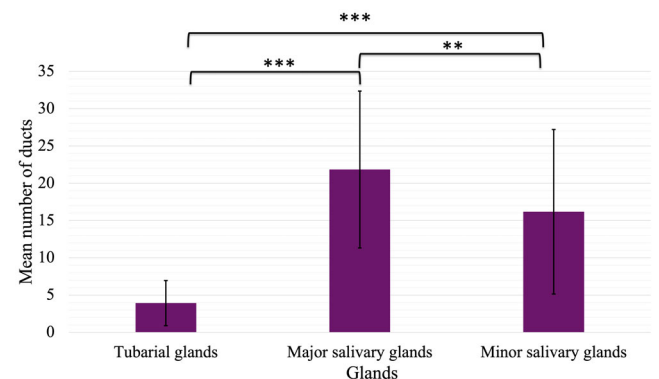


FIGURE 4 Mean number of ducts in one high-power field of view. Major salivary glands have the most ducts and tubarial glands have the least ducts. Data are reported as means and error bars represent standard deviation. $n = 8$ male donors and 3 female donors. A one-way ANOVA was used to compare combined male and female values between all the glands. *** $p < 0.0001$ and ** $p < 0.0006$.

TABLE 4 Mucinous acini area.

Glands	Mean mucinous acini area \pm standard deviation		
	Combined male and female (μm^2)	Male (μm^2)	Female (μm^2)
Sublingual glands	$1.2 \times 10^3 \pm 0.5 \times 10^3$	$1.0 \times 10^3 \pm 0.4 \times 10^3$	$1.5 \times 10^3 \pm 0.5 \times 10^3$
Submandibular glands	$1.2 \times 10^3 \pm 0.6 \times 10^3$	$0.9 \times 10^3 \pm 0.2 \times 10^3$	$1.6 \times 10^3 \pm 0.7 \times 10^3$
Buccal glands	$3.0 \times 10^3 \pm 2.0 \times 10^3$	$2.9 \times 10^3 \pm 2.2 \times 10^3$	$3.2 \times 10^3 \pm 1.5 \times 10^3$
Labial glands	$2.4 \times 10^3 \pm 0.9 \times 10^3$	$2.3 \times 10^3 \pm 0.7 \times 10^3$	$2.5 \times 10^3 \pm 0.1 \times 10^3$
Tubarial glands	$3.2 \times 10^3 \pm 1.3 \times 10^3$	$4.1 \times 10^3 \pm 1.1 \times 10^3$	$2.2 \times 10^3 \pm 0.7 \times 10^3$

Note: Data are reported as means and standard deviation. $n = 2$ male donors and 2 female donors. For each gland, the area of 10 acini within 1 field of view at $100\times$ (0.76 mm^2) was found from every donor. The buccal glands from 1 female donor were not included due to more extensive acinar atrophy than all other samples.

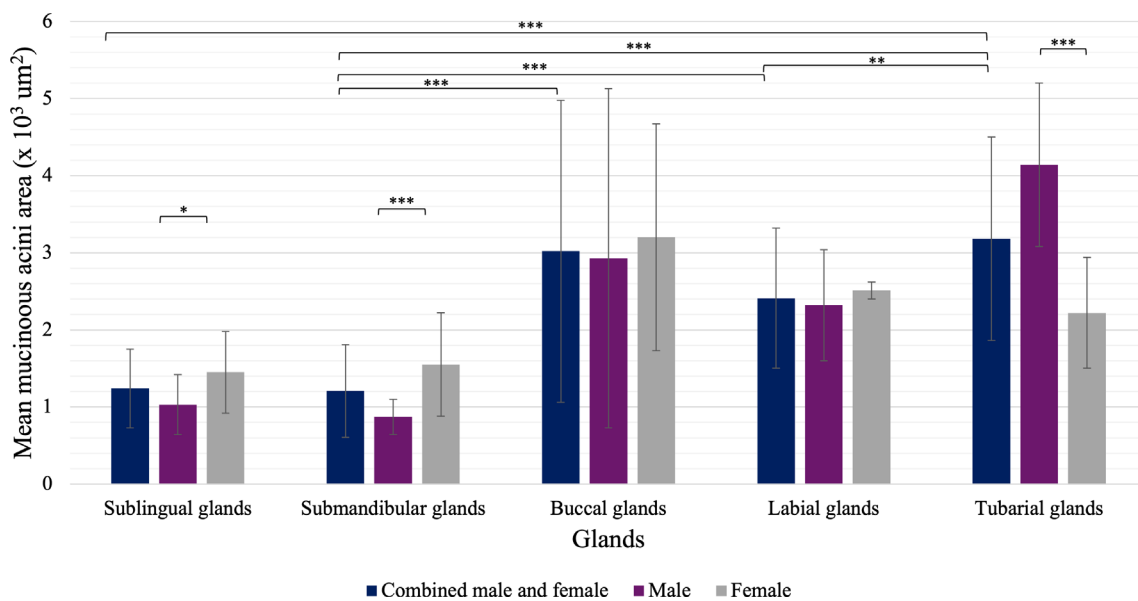


FIGURE 5 Mean mucinous acini area in one high-power field of view. The mean mucinous acini area of the tubarial glands (TG) is similar to the buccal glands. The submandibular glands had a smaller mean mucous acini area compared with the buccal and labial glands. The mean mucous acini area of the TGs is higher in males than females. Data are reported as means and error bars represent standard deviation. $n = 2$ male donors and 2 female donors. The buccal glands from 1 female donor were not included due to more extensive acinar atrophy than all other samples. A two-tailed unpaired t-test was used to compare the glands between males and females (within gland comparison). A one-way ANOVA was used to compare combined male and female values between all the glands. $*p < 0.05$, $**p < 0.01$ and $***p < 0.001$.

lobule ($p = 0.8632$). The results are summarized in Table 2 and Figure 3.

3.1.3 | Number of ducts

The mean number of ducts in the major SGs was greater than the TGs ($p < 0.0001$) and minor SGs ($p < 0.0006$). The mean number of ducts of the minor SGs was significantly greater than the TGs ($p < 0.0001$). The results are summarized in Table 3 and Figure 4.

3.1.4 | Area of the mucinous acini

In both male and female samples, the TGs have the greatest mean mucinous acini area, which is greater than the mean mucinous acini area of the sublingual glands and submandibular glands ($p < 0.001$ and $p < 0.01$ respectively). The mean mucinous acini area of the TGs resembles the buccal glands. The submandibular glands of both male and female samples have the smallest mean mucinous acini area, which is smaller than the mean mucinous acini area of the buccal and labial glands ($p < 0.001$).

TABLE 5 Number of mucinous acini.

Glands	Mean number of mucinous acini \pm standard deviation		
	Combined male and female	Male	Female
Sublingual glands	133.8 \pm 55.2	162.0 \pm 21.2	105.5 \pm 74.2
Submandibular glands	42.5 \pm 19.5	58.5 \pm 10.6	26.5 \pm 2.1
Buccal glands	54.3 \pm 34.5	49.5 \pm 47.4	64.0 \pm 0.0
Labial glands	61.0 \pm 32.1	68.5 \pm 46.0	53.5 \pm 27.6
Tubarial glands	82.0 \pm 30.4	102.0 \pm 14.1	62.0 \pm 31.1

Note: Data are reported as raw numbers of acini and standard deviation. $n = 2$ male donors and 2 female donors. For each gland, the number of acini within an area of 0.36 mm² was found from every donor. The buccal glands from 1 female donor were not included due to more extensive acinar atrophy than all other samples.

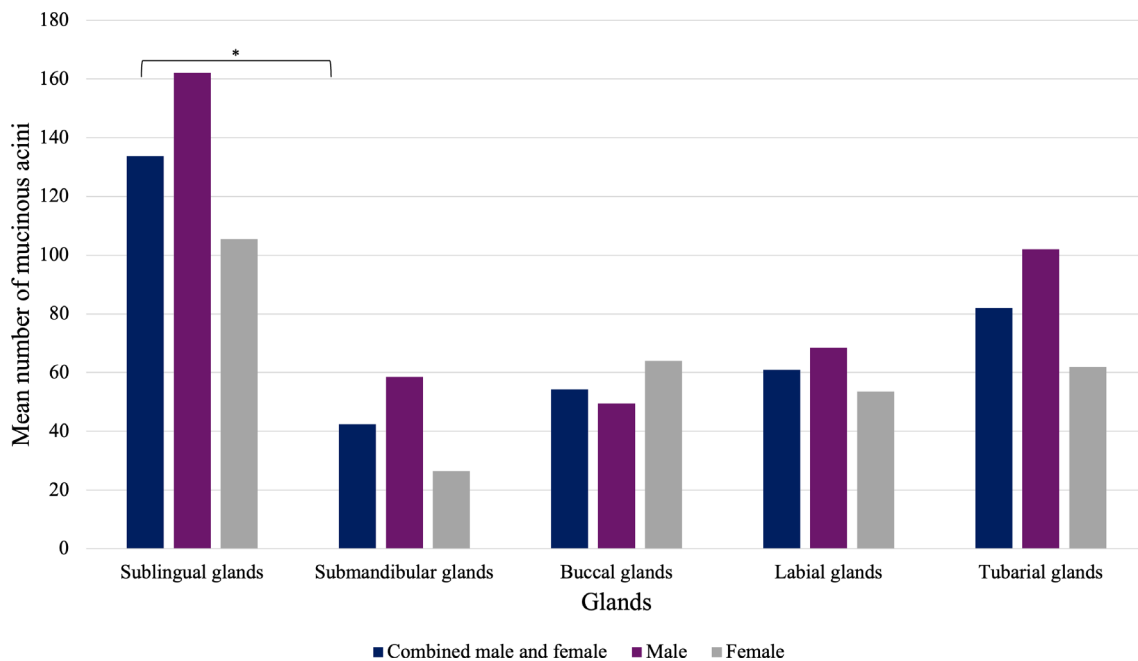


FIGURE 6 Mean number of mucinous acini in one high-power field of view. Sublingual glands have the highest number of mucinous acini. Data are reported as means and error bars represent standard error of the mean. $n = 2$ male donors and 2 female donors. The buccal glands from 1 female donor were not included due to more extensive acinar atrophy than all other samples. A one-way ANOVA was used to compare combined male and female values between all the glands. $*p < 0.05$.

The mean mucinous acini area of the submandibular glands is similar to the sublingual glands.

Within our cohort of donors, in some SGs, the mucinous acini area has sex-based differences. In the sublingual glands, the mean mucinous acini area is greater in females compared with males ($p < 0.05$). In the submandibular glands, the mean mucinous acini area is also greater in females compared with males ($p < 0.001$). Furthermore, in the TGs the mean mucinous acini area is greater in males compared with females ($p < 0.001$). All parameters are normalized to the donor body mass index. The results are summarized in Table 4 and Figure 5.

3.1.5 | Number of mucinous acini

In both male and female samples, the sublingual glands have the greatest number of mucinous acini, which is greater than the submandibular glands ($p < 0.05$) and similar to all of the other glands. Additionally, the submandibular glands have a similar number of mucinous acini to the minor SGs and TGs. The TGs, sublingual and submandibular glands have a similar number of mucinous acini. No significant differences exist between male and female samples for any of the glands. The results are summarized in Table 5 and Figure 6.

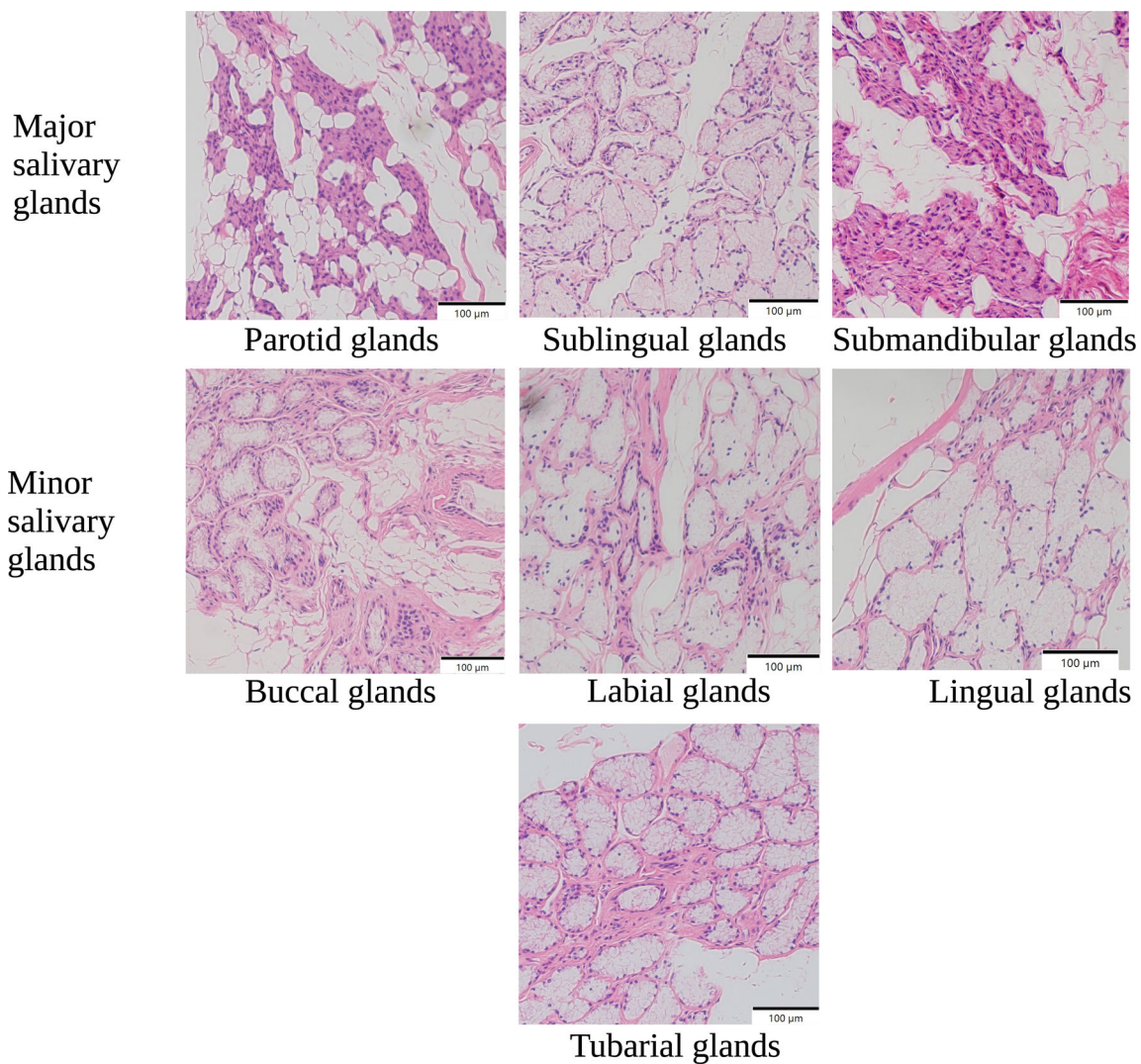


FIGURE 7 Representative images of the histology of all the dissected glands (parotid, sublingual, submandibular, buccal, labial, lingual, and tubarial glands [TGs]). TGs contain densely packed clusters of predominantly mucinous acini surrounded by loose connective tissue resembling minor SGs. All images are taken at 100 \times . Scale bar is 100 μ m.

3.2 | Qualitative results

All the major and minor SGs were successfully dissected from 11 donors and their histological architecture was analyzed qualitatively (Figure 7). In general, when dissecting all SGs, we consistently observed the major SGs lacking any distinct fascia encapsulating the entire glandular tissue.

The glandular tissue found within the TG region of both male and female donors is observationally comprised primarily of mucinous acini with a minor serous component connected by excretory salivary ducts (Figure 8a). Moreover, we observed that in some samples, the ducts of the buccal and labial glands merge perpendicularly with the mucosal surface, whereas in the TGs, the ducts merge with the mucosal surface at a

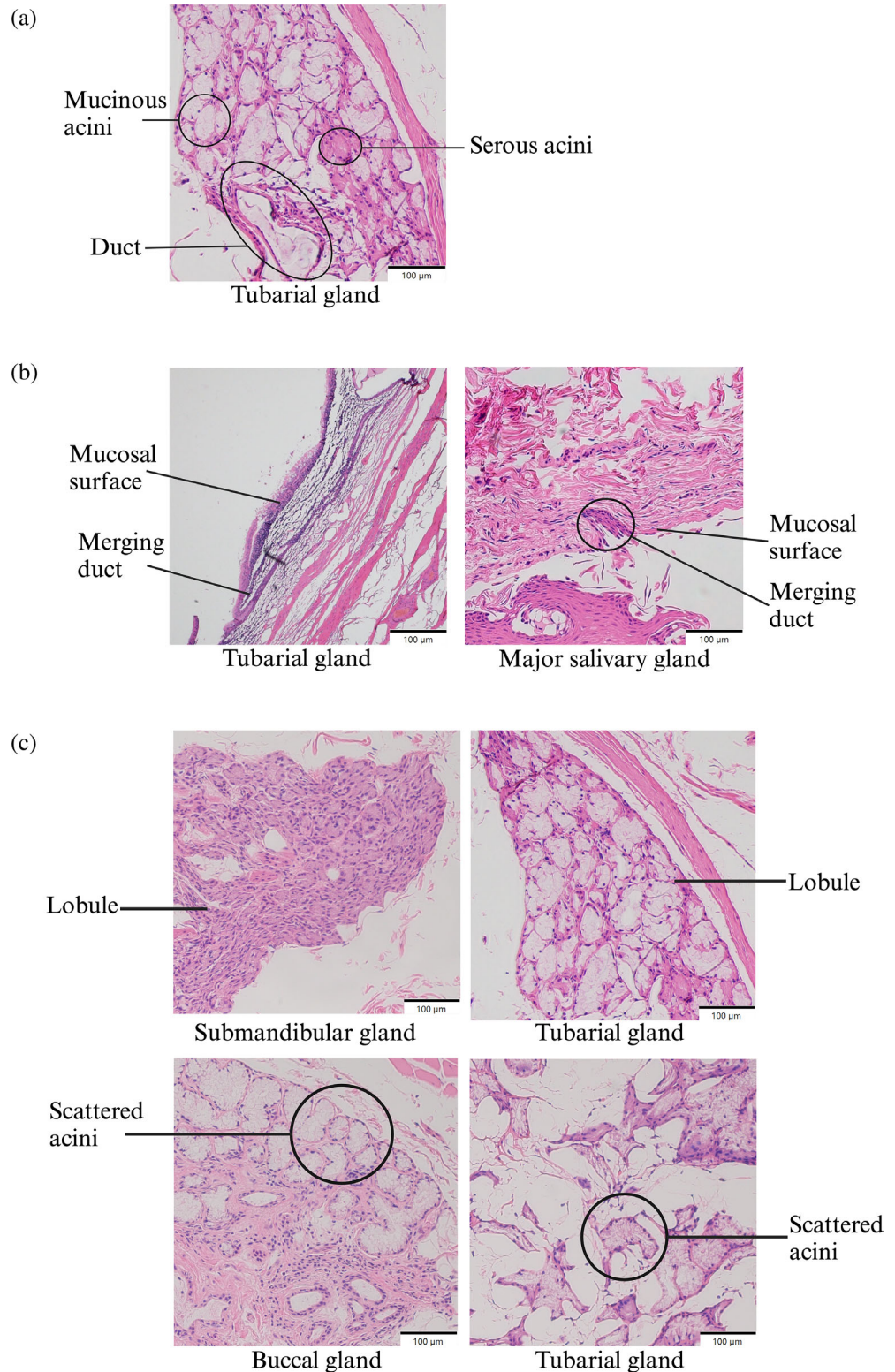
20–30° angle (Figure 8b). The glandular tissue found in the TGs is organized in 2 ways: first, the TGs display lobular acini architecture in some regions. Second, the TGs also display scattered acini without distinct organization in some regions (Figure 8c). Finally, in the TGs, the acini density is greater when proximal to regions of cartilage when compared with regions more proximal to the mucosal surface.

4 | DISCUSSION

Quantitatively, the tissue architecture of TGs resembles the minor SGs. TGs contain densely packed clusters of predominantly mucinous acini surrounded by loose connective tissue. Additionally, the TGs and minor SGs have

FIGURE 8 Tubarial gland (TG) qualitative findings.

(a) Glandular tissue found in the TGs, containing a duct, serous acini, and mucinous acini.
 (b) Duct orientation when merging with the mucosal surface between the TGs. In the TGs, ducts merge with the mucosal surface at an angle, compared with the salivary glands (SGs), which have ducts that merge with the mucosal surface perpendicularly.
 (c) Acini organization in the TGs compared with the major and minor SGs. Some regions of the TGs display both the highly organized, lobular acinar architecture more commonly seen in the major SGs and the less organized, scattered acinar structure seen typically in the minor SGs. All images were taken at 100 \times . Scale bar is 100 μ m.



similar lobule areas. Furthermore, the average total glandular area in the TGs is similar to that of the minor SGs. The TGs have a lower number of ducts than the major SGs and the minor SGs. However, qualitatively, the TGs are unique from both the major and minor SGs in several aspects. In some regions, the TGs have ducts that run

parallel to the mucosal surface and a terminal end that merges with the mucosal surface at an angle, which makes them stand out from the major and minor SGs, whose ducts merge with the mucosal surface perpendicularly. Some regions of the TGs display both the highly organized, lobular acinar architecture more commonly seen in

the major SGs and the less organized, scattered acinar structure seen typically in the minor SGs (Gupta & Ahuja, 2019; Tani & Skoog, 2008). Although the quantitative results may not directly reflect what would be seen in the glands of a living population, the comparisons made between the embalmed glands likely reflect the reality which would infer the structure and function of the living glands.

The TGs are packed with predominantly mucinous acini and can release mucinous fluid that coats and moistens the mucosal surface of the pharynx. They are located at the posterior–superior aspect of the nasopharynx, serving as a spout of glandular tissue, and with the assistance of gravity, can effectively provide protective coverage to a large area of the pharynx by modulating environmental pH and immune interactions (Brunworth et al., 2014; Takano et al., 2022). Based on the TG's size, density, and location, they are the predominant glandular tissue in the pharyngeal region that can provide enough secretion for mucosal protection. Radiotherapy (RT) is an important and effective cancer therapy using intense X-ray energy exposure; however, when administered to the head and neck region can result in atrophy of the SGs, leading to complications such as xerostomia (dry mouth) and dysphagia (difficulty eating due to issues with mastication and swallowing) (Neville et al., n.d.; Fillit et al., 2010; Valstar et al., 2021). Currently, the organs at risk (namely the major SGs) are protected before a patient undergoes RT by administering a lower radiation dose to that region or by using a protective agent such as amifostine (Neville et al., n.d.; Chao, 2002; Fillit et al., 2010; Valstar et al., 2021). However, despite this SG protection, some patients still experience xerostomia and dysphagia post-RT (Neville et al., n.d.; Fillit et al., 2010; Valstar et al., 2021). In these cases, the xerostomia and dysphagia may be the result of the collateral damage to the unprotected TGs (Valstar et al., 2021). Our study supports the need for further investigation into how TGs should be effectively protected when designing the radiation fields and intensity used to treat head and neck cancers to reduce or prevent post-RT complications. In addition to the effects of RT, the TGs might also contribute as the source of SG tumors. Although primary SG tumors are rare, the types of tumors developed primarily from the major SGs are different from those developed from the minor SGs (Guzzo et al., 2010; Pinkston & Cole, 1999). For example, Warthin's tumor is only seen in the parotid gland, whereas hyalinizing clear cell carcinoma is only seen in the minor SG regions (Zhai et al., 2023). These differences in the types of tumors developed in the major and minor SGs display the importance of considering histology when applying new anatomical findings clinically.

Sexual dimorphism was observed in the mean mucinous acini area between male and female TGs. Sex-based differences were also observed in the mean mucinous acini area between male and female submandibular and sublingual glands. Females had greater mucinous acini areas in the sublingual glands and submandibular glands, whereas males had greater mucinous acini areas in the TGs. There is no uniformity across all the glands for whether males or females had greater mucinous acini areas. These differences, albeit interesting, could be potentially due to individual variability and can be addressed in future work using SG tissue samples stored in a biobank at the University of Calgary. Despite the validity of these sex-based differences being unknown, these findings do shed light on the importance of addressing this gap in knowledge. Previous literature has found few structural differences between male and female SGs (Inoue et al., 2006; Moreira et al., 2006; Rosa et al., 2020). Inoue et al. (2006) used MRI to find that in their donor population (likely predominantly Japanese), males had larger parotid and submandibular glands compared with females. Additionally, Rosa et al. (2020) found that in their donor population (likely predominantly South American), the accessory parotid gland was more commonly unilateral in males and bilateral in females. This study shows that sex-based histological differences are not only relevant for the TGs but are also relevant for other SGs. These findings have potential clinical implications, as acknowledging that sex-based and ethnic differences can support the development of management plans that are more aligned with the individual's own anatomy. In addition to the anatomical variability already discussed, Pinna et al. (2015) found that females had lower secretion rates from the buccal and labial glands, lower whole saliva secretion rates, and lower levels of IgA in the buccal saliva compared with males. These differences in salivation rates are potential reasons why females have higher rates of xerostomia compared with males (Furness et al., 2013). By understanding the functional and sexual dimorphism in SGs and salivation, we can adapt our management plans to provide more specific RT protection for higher-risk female patients.

Currently, there are 3 main criteria for distinguishing the major and minor SGs, none of which are quantitative and comprehensive (Kessler & Bhatt, 2018; Tani & Skoog, 2008). These criteria are: (Basbaum et al., 1990) the major SGs contain an extensive ductal branching system, (Tucker, 2007) the major SGs are larger, and can therefore be visualized on standard radiological images such as MRI, and (Lee et al., 2012) the major SGs have more highly organized, lobular acini arrangements compared

with the minor SGs (Gupta & Ahuja, 2019; Kessler & Bhatt, 2018; Tani & Skoog, 2008). Our findings critically evaluate these criteria and bring their use in the classification of SGs into discussion. First, the major SGs are categorized by their extensive ductal branching (Gupta & Ahuja, 2019; Tani & Skoog, 2008). The number of ducts in the TGs is lower than in both the major and minor SGs, proposing that the TGs being major SGs are unlikely. It should be noted that it is difficult to definitively discern if the observed ducts were unique to one another, or if they were cross-sections of the same duct weaving in and out of the tissue. Nevertheless, increased duct branching could theoretically be inferred through a greater number of individual ducts, and through tortuous ducts weaving in and out of a region (Ghannam & Singh, 2021).

Second, the major SGs are categorized by being easily visible on standard radiological images such as MRI, whereas the minor SGs are not (Kessler & Bhatt, 2018). Similar to the minor SGs, the TGs are not easily visualized on MRI scans and appear as shadowy regions of soft tissue, which are difficult to discern from the surrounding tissue (Valstar et al., 2021). The relative ease of visualizing major SGs compared with minor SGs is due to the size of the glands and their location. This is because the major SGs are large glands that occupy a specific anatomical location but the minor SGs are minute glands scattered throughout the upper aerodigestive tract (Treuting et al., 2018). However, all SGs, the prostate gland, and the kidneys can be visualized clearly by PSMA PET/CT incidentally. It is possible that the high PSMA PET/CT signal stemming from the TG region is not due to the existence of a singular major SG, but rather due to a high density of minor SGs that are closely packed together and appear as separate masses.

Third, the major SGs are distinguished by having more highly organized, lobular acini arrangements compared with the minor SGs. Histologically, we observed that the TGs are most similar to the minor SGs while displaying some unique features that distinguish themselves from both major and minor SGs. Taking all SGs' histological architecture into consideration, we propose that the histological characteristics of all SGs are better organized along a spectrum depending on the parameter being analyzed. Organization along a spectrum would account for the TGs sharing similarities with the major and minor SGs when looking at mucinous acini and duct density and would also account for the TGs falling intermediate between the major and minor SGs when looking qualitatively at their structure, while also possessing some qualities which make the TGs stand out from both the major and minor SGs. Based on our observations regarding SG

criteria and the analysis of TGs and SGs, we propose that the TGs should be classified as minor SGs; however, the classification of SGs into two discrete groups is not comprehensive. Instead, histological, functional, and imaging-based criteria should be considered in combination when analyzing and categorizing SGs.

In addition to these criteria, many sources state that the major SGs are surrounded by a fibrous fascia capsule (Ghannam & Singh, 2021; Gupta & Ahuja, 2019; Riva et al., 1990). However, we found no gross or microscopic evidence of encapsulation of the major SGs. The parotid and submandibular glands are abutted by deep cervical fascia on one aspect but are not themselves encapsulated, and the sublingual glands have no fascia on any aspect. This lack of fascia has been observed in hundreds of surgical and biobank samples at our center, and therefore, the absent fascia is not due to an artifact of tissue collection and processing.

In this study, we observed sex-based differences in the TGs and SGs, which could be used to help explain sex-based differences in salivation, as well as for more targeted SG sparing for RT. We proposed more comprehensive criteria and approaches to categorize SGs to better encompass the histological nuances that exist. Taken together, these findings provide detailed histological analysis on an understudied cluster of SGs, and valuable information that can assist in the design and delivery of treatment for head and neck cancers. However, unanswered questions remain regarding the reason and the physiological and clinical implications for the high PSMA uptake by the TGs. Understanding this high PSMA uptake might provide a better understanding of how the TGs function and their contribution to various head and neck pathologies. Additionally, the TGs' hypothesized role in head and neck cancers, both as a potential cause of xerostomia and dysphagia and as a primary tumor site for head and neck cancers is also unanswered. Overall, this study provides a much-needed quantitative and sex-based histological analysis of the SGs and the recently characterized TGs, which opens new avenues for exploration in areas of pharyngeal arch development and SG tumor development in the future.

AUTHOR CONTRIBUTIONS

Alisha Ebrahim: Conceptualization; investigation; writing – original draft; methodology; visualization; writing – review and editing; formal analysis; project administration; data curation. **Caitlan Reich:** Investigation; data curation; funding acquisition; methodology; project administration; visualization; writing – review and editing. **Kurt Wilde:** Investigation; writing – review and editing; visualization; formal analysis.

Aly Muhammad Salim: Investigation; writing – review and editing; formal analysis. **Martin D. Hycza:** Funding acquisition; conceptualization; methodology; project administration; resources; supervision; validation; writing – review and editing. **Lian Willetts:** Conceptualization; funding acquisition; methodology; project administration; resources; supervision; validation; writing – review and editing.

ACKNOWLEDGMENTS

We would like to thank the staff at the Advanced Technical Skills Simulation Laboratory (ATSSL) at the Cumming School of Medicine for their support. Images were generated by the authors using BioRender software. [Correction added after first online publication on 18 September 2024. Acknowledgments has been updated.]

FUNDING INFORMATION

This work was supported by the University of Calgary Department of Pathology and Laboratory Medicine Trainee-Led Project Support Initiative and Department of Cell Biology & Anatomy, Faculty of Medicine, University of Calgary.

CONFLICT OF INTEREST STATEMENT

The authors do not have any conflict of interest to disclose.

ORCID

Alisha Ebrahim  <https://orcid.org/0000-0002-6627-5184>

REFERENCES

- Anderson, S. D. (2006). Practical light embalming technique for use in the surgical fresh tissue dissection laboratory. *Clinical Anatomy*, 19(1), 8–11.
- Basbaum, C. B., Jany, B., & Finkbeiner, W. E. (1990). The serous cell. *Annual Review of Physiology*, 52(1), 97–113.
- Brunworth, J. D., Mahboubi, H., Garg, R., Johnson, B., Brandon, B., & Djalilian, H. R. (2014). Nasopharyngeal acid reflux and Eustachian tube dysfunction in adults. *The Annals of Otolaryngology, Rhinology, and Laryngology*, 123(6), 415–419.
- Chao, K. S. (2002). Protection of salivary function by intensity-modulated radiation therapy in patients with head and neck cancer. *Seminars in Radiation Oncology*, 12(1 Suppl 1), 20–25.
- Fillit, H. M., Rockwood, K., & Woodhouse, K. (2010). Malnutrition in older adults. In *Brocklehurst's textbook of geriatric medicine and gerontology* (7th ed., pp. 949–958). Elsevier.
- Formenti, S. C., & Demaria, S. (2009). Systemic effects of local radiotherapy. *The Lancet Oncology*, 10(7), 718–726.
- Furness, S., Bryan, G., McMillan, R., Birchenough, S., & Worthington, H. V. (2013). Interventions for the management of dry mouth: Non-pharmacological interventions. *Cochrane Database of Systematic Reviews*, 2013(9), CD009603.
- Ghannam, M. G., & Singh, P. (2021). *Anatomy, head and neck, salivary glands*. StatPearls Publishing. <https://www.ncbi.nlm.nih.gov/books/NBK538325/?report=classic>
- Gilloteaux, J., & Afolayan, A. (2014). Clarification of the terminology of the major human salivary glands: Acinus and alveolus are not synonymous. *The Anatomical Record*, 297(8), 1354–1363.
- Gupta, S., & Ahuja, N. (2019). *Salivary glands*. IntechOpen.
- Guzzo, M., Locati, L. D., Prott, F. J., Gatta, G., McGurk, M., & Licitra, L. (2010). Major and minor salivary gland tumors. *Critical Reviews in Oncology/Hematology*, 74(2), 134–148.
- Hsieh, M.-S., Jeng, Y.-M., Jhuang, Y.-L., Chou, Y.-H., & Lin, C.-Y. (2016). Carbonic anhydrase VI: A novel marker for salivary serous acinar differentiation and its application to discriminate acinic cell carcinoma from mammary analogue secretory carcinoma of the salivary gland. *Histopathology*, 68(5), 641–647.
- Hukkanen, R. R., Dintzis, S. M., & Treuting, P. M. (2018). 8—salivary glands. In P. M. Treuting, S. M. Dintzis, & K. S. Montine (Eds.), *Comparative anatomy and histology* (2nd ed., pp. 135–145). Academic Press.
- Inoue, H., Ono, K., Masuda, W., Morimoto, Y., Tanaka, T., Yokota, M., & Inenaga, K. (2006). Gender difference in unstimulated whole saliva flow rate and salivary gland sizes. *Archives of Oral Biology*, 51(12), 1055–1060.
- Kessler, A. T., & Bhatt, A. A. (2018). Review of the major and minor salivary glands, part 1: Anatomy, infectious, and inflammatory processes. *Journal of Clinical Imaging Science*, 8, 47.
- Lee, M. G., Ohana, E., Park, H. W., Yang, D., & Muallem, S. (2012). Molecular mechanism of pancreatic and salivary gland fluid and HCO₃ secretion. *Physiological Reviews*, 92(1), 39–74.
- Moreira, C. R., Azevedo, L. R., Lauris, J. R., Taga, R., & Damante, J. H. (2006). Quantitative age-related differences in human sublingual gland. *Archives of Oral Biology*, 51(11), 960–966.
- Neville, B., Damm, D. D., Allen, C., & Chi, A. (2018). *Physical and chemical injuries. Color atlas of oral and maxillofacial diseases* (1st ed., pp. 169–203). Elsevier.
- Ottone, N., Vargas, C. A., Fuentes, R., & Sol, M. (2016). Walter Thiel's embalming method. Review of solutions and applications in different fields of biomedical research. *International Journal of Morphology*, 34, 1442–1454.
- Pinkston, J. A., & Cole, P. (1999). Incidence rates of salivary gland tumors: Results from a population-based study. *Otolaryngology and Head and Neck Surgery*, 120(6), 834–840.
- Pinna, R., Campus, G., Cumbo, E., Mura, I., & Milia, E. (2015). Xerostomia induced by radiotherapy: An overview of the physiopathology, clinical evidence, and management of the oral damage. *Therapeutics and Clinical Risk Management*, 11, 171–188.
- Riva, A., Lantini, M. S., & Riva, F. T. (1990). Normal human salivary glands. In A. Riva, P. M. Motta, & F. T. Riva (Eds.), *Ultrastructure of the extraparietal glands of the digestive tract* (pp. 53–74). Springer US.
- Rosa, M. A., Łazarz, D. P., Pękala, J. R., Skinningsrud, B., Lauritzen, S. S., Solewski, B., Pękala, P. A., Walocha, J. A., & Tomaszewski, K. A. (2020). The accessory parotid gland and its clinical significance. *The Journal of Craniofacial Surgery*, 31(3), 856–860.
- Takano, K., Kurose, M., Kamekura, R., Kanda, M., Yamamoto, M., & Takahashi, H. (2022). Tubarial gland involvement in IgG4-related diseases. *Acta Oto-Laryngologica*, 142(7–8), 616–619.

- Tani, E. M., & Skoog, L. (2008). Salivary glands and rare head and neck lesions. In M. Bibbo & D. Wilbur (Eds.), *Comprehensive cytopathology* (3rd ed., pp. 607–632). W.B. Saunders.
- Treuting, P. M., Morton, T. H., & Vogel, P. (2018). Oral cavity and teeth. In P. M. Treuting, S. M. Dintzis, & K. S. Montine (Eds.), *Comparative anatomy and histology* (2nd ed., pp. 115–133). Academic Press.
- Tucker, A. S. (2007). Salivary gland development. *Seminars in Cell & Developmental Biology*, 18(2), 237–244.
- Turk, A. (2020). Tubarial or not to be—A potential new organ in the pharynx. *Cell Pathology*, 6(1), 3–4.
- Valstar, M. H., de Bakker, B. S., Steenbakkers, R., de Jong, K. H., Smit, L. A., Klein Nulent, T. J. W., van Es, R. J. J., Hofland, I., de Keizer, B., Jasperse, B., Balm, A. J. M., van der Schaaf, A., Langendijk, J. A., Smeele, L. E., & Vogel, W. V. (2021). The tubarial salivary glands: A potential new organ at risk for radiotherapy. *Radiotherapy and Oncology*, 154, 292–298.
- Washington University School of Medicine Neuromuscular Lab. (1997). *Hematoxylin & eosin (H & E) stain protocol*. Washington University School of Medicine Neuromuscular Lab.
- Zhai, C., Yuan, C., Sun, J., Song, W., Wang, S., & Lin, L. (2023). Clinical and histopathologic analyses of nasopharyngeal Hyalinizing clear cell carcinoma: A series of 26 cases with molecular confirmation. *The American Journal of Surgical Pathology*, 47(10), 1168–1175.

SUPPORTING INFORMATION

Additional supporting information can be found online in the Supporting Information section at the end of this article.

How to cite this article: Ebrahim, A., Reich, C., Wilde, K., Salim, A. M., Hyrcza, M. D., & Willetts, L. (2025). A comprehensive analysis of the tubarial glands. *The Anatomical Record*, 308(5), 1425–1437. <https://doi.org/10.1002/ar.25561>